

Sawtooth Control Relying on Toroidally Propagating ICRF Waves

J. P. Graves 1), I. T. Chapman 2), S. Coda 1), T. Johnson 3), M. Lennholm 4), B. Alper 2), M. de Baar 5), K. Crombe 6), L.-G. Eriksson 7), R. Felton 2), D. Howell 2), V. Kiptily 2), H. R. Koslowski 8), M.-L. Mayoral 2), I. Monakhov 2), I. Nunes 9), S. D. Pinches 2) and JET-EFDA contributors*

JET-EFDA, Culham Science Centre, OX14 3DB, Abingdon, UK

1) École Polytechnique Fédérale de Lausanne (EPFL), Centre de Recherches en Physique des Plasmas (CRPP), Association EURATOM-Confédération Suisse, 1015 Lausanne, Switzerland

2) Euratom/CCFE Fusion Association, Culham Science Centre, Abingdon, UK

3) Euratom-VR Association, EES, KTH, Stockholm, Sweden

4) EFDA-JET CSU, Culham Science Centre, Abingdon, OX14 3DB, UK

5) FOM Instituut voor Plasmafysica Rijnhuizen, Association EURATOM-FOM, The Netherlands

6) Department of Applied Physics, Ghent University, Rozier 44, 9000 Ghent, Belgium

7) European Commission, Directorate General for Research, Unit J4 - Fusion Assoc. Agreement

8) Forschungszentrum Jülich GmbH Institut für Energieforschung - Plasmaphysik, Germany

9) Associação EURATOM/IST, 1049-001, Lisboa, Portugal

E-mail contact of main author: jonathan.graves@epfl.ch

Abstract. Dedicated JET experiments have been devised in order to test the predictions of a recent theory [J. P. Graves, *et al.*, Phys. Rev. Lett. **102**, 065005 (2009)] indicating that sawteeth can be destabilised by ICRH in reactor relevant conditions. Energetic passing ions influence the MHD internal kink mode instability when they are distributed asymmetrically in parallel velocity, which is a natural feature of minority ion populations in resonance with toroidally co or counter propagating ICRF waves. Reported here are theory and dedicated JET experiments which have been devised in order to neutralise an alternative sawtooth control mechanism, involving changes in the equilibrium current due to ICRF, and permit comparison with recent theory across physical parameters. Negligible change to the net equilibrium current was assured by choosing ITER relevant ^3He minority ICRF. Depending on the antenna phasing, the sawtooth period can remain as short as those of Ohmic pulses, despite being close to the L-H threshold. A change of antenna phasing can produce sawteeth so long that NTMs are triggered and saturated even in L-mode. The sawtooth stability properties are explained by the effect of the wide drift orbits of fast ions intersecting the $q = 1$ radius. Sophisticated numerical modelling agrees well with an analytical solution involving the distribution of energetic particles at $q = 1$, and with salient experimental observation.

1. Introduction

It is now well known that long period sawteeth can trigger neoclassical tearing modes (NTMs) even in plasmas with quite moderate performance. This is clearly a concern for future standard operation in ITER because the alpha particle population could lengthen the sawteeth period by up to 100s [1]. To put this into perspective, Fig. 1 reproduces a recent study [2] showing the normalised beta β_N in various machines at the time when a sawtooth triggered an NTM, plotted with respect to the sawtooth period normalised to the resistive diffusion. The data selected from expected ITER like parameters (shape, auxiliary power relative to L-H threshold power) demonstrates significant data collapse across machine parameters. Assuming that this data collapse would hold also for ITER, it is possible to predict the onset beta in ITER for an estimate of the resistive time and a chosen value of the sawtooth period (10s and 100s chosen in Fig. 1).

It is clear from Fig. 1 that we would wish to avoid sawteeth of 100s in ITER, where we predict NTM triggering at only $\beta_N \approx 1.5$. In the present paper, we show that NTMs can be triggered even in L-mode with $\beta_N \approx 0.8$ by very long sawteeth. One particular JET pulse examined here, 78739, shown in detail in Fig. 2, collapses on to the data set, and is seen, in Fig. 1 to be the largest normalised sawtooth period and smallest normalised beta. The auxiliary power,

*See the Appendix of F. Romanelli et al., paper OV/1-3, this conference

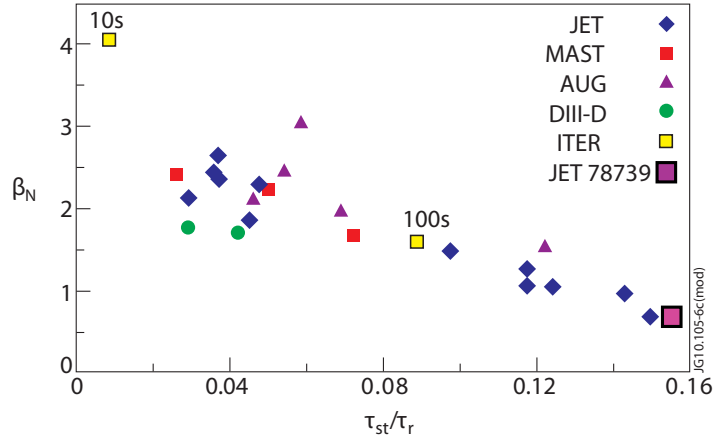


FIG. 1. Showing the normalised beta at the time of a sawtooth triggered NTM in various tokamaks, plotted as a function of the sawtooth period normalised to the resistive diffusion time [2]. Assuming similar data collapse in ITER it is possible to predict the critical normalised beta for a particular guess of the sawtooth period. Figure partially reproduced from Fig. 6 of Ref. [I. T. Chapman, *Nucl. Fusion* **50** 102001 (2010)]. Copyright rests with Euratom.

relative to that required for L-H transition, was lower in 78739 than the lower limit of the original data set employed in Ref. [2]. Nevertheless, this particular pulse fitted into the remit of sawtooth control and manipulation in the set of experiments reported here, whose primary aim was to validate a recent theory describing the mechanism of sawtooth control using ICRH, and to do this using ITER relevant minority ^3He . The highly effective nature of sawtooth control using toroidally propagating ICRF waves with off-axis resonance in tokamaks has recently been explained [3]. Energetic passing ions influence the MHD internal kink mode instability when they are distributed asymmetrically in parallel velocity. Such populations are generated by toroidally aligned NBI, and its effect on sawteeth is well documented [4, 5], but parallel velocity asymmetry is also a natural feature of minority ion populations in resonance with toroidally co or counter propagating ICRF waves. This paper reports the theory [3] and dedicated JET experiments [6] which have been devised in order to neutralise an alternative sawtooth control mechanism [7, 8], involving changes in the equilibrium current due to ICRF [9, 7, 10], and permit comparison with recent theory [3] across physical parameters. Negligible change to the net equilibrium current was assured [6] by choosing ITER relevant ^3He minority ICRF.

The effectiveness of minority ^3He ICRF for controlling sawteeth, and its importance, is illustrated in Fig. 2. The difference between the two pulses is that the direction of the toroidally propagating ICRF waves is counter-tangent to the plasma current in pulse 78737 (-90° antenna phasing), and co-tangent ($+90^\circ$ antenna phasing) in 78739, which is the JET pulse indicated by the bold square in Fig. 1. In both pulses the early NBI phase increases the sawtooth period to 300ms from Ohmic sawteeth of around 80ms. At 18s, 4.5MW of ^3He ICRF is applied on the high field side of the $q = 1$ rational surface. A very slow ramp in the magnetic field and current gives rise to a minimum in the sawtooth period of 100ms for the -90° phasing pulse, while for $+90^\circ$ phasing the sawteeth become extremely long. A sawtooth of more than 1 second triggers a neoclassical tearing mode (NTM), as indicated by the $n = 2$ toroidal mode number magnetic signal shown in Fig. (2). That this could happen despite the pulse being in L-mode particularly highlights the crucial importance of sawtooth control.

2. Theoretical Development

In this section we identify [3] the effects of finite orbit widths and parallel velocity asymmetry for an arbitrary distribution function. We write down a solution [11] to the perturbed distribution

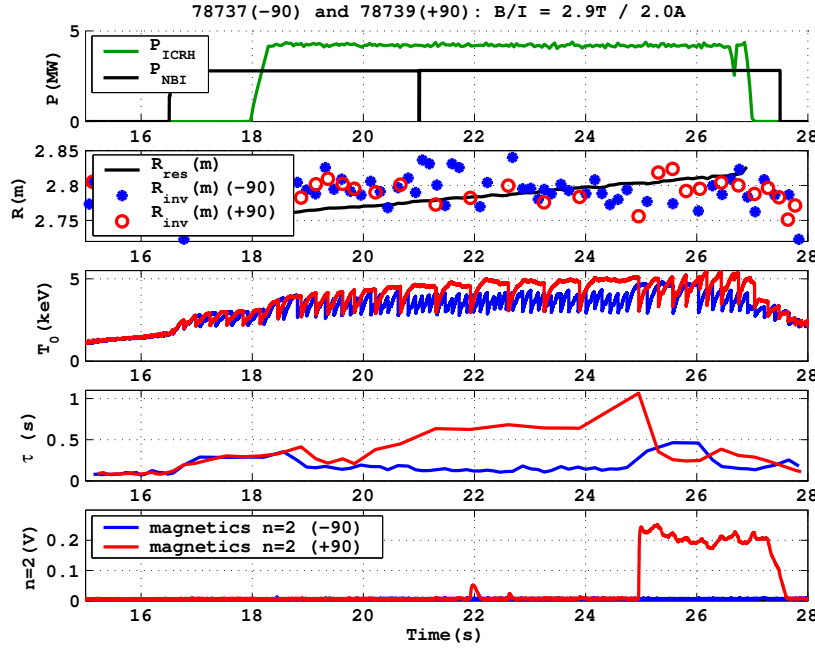


FIG. 2. Time traces of 78737 (blue, -90° phasing) and 78739 (red, $+90^\circ$ phasing). Reproduced from Fig. 1 of Ref. [J. P. Graves, et al, Nucl. Fusion **50** 052002 (2010)]. Copyright rests with Euratom.

function $\delta F = \delta F_f + \delta F_k$ which treats wide radial drift excursion. From Refs. [11]:

$$\delta F_f = -(Ze/m)(\underline{\xi} \cdot \underline{\nabla} \psi_p) \frac{\partial F}{\partial \mathcal{P}_\phi} \quad (1)$$

is the adiabatic (fluid) contribution, $\underline{\xi} = \hat{\underline{\xi}} \exp(-in\phi - i\omega t)$ is the MHD displacement with $\hat{\underline{\xi}} = \sum_m \hat{\underline{\xi}}_m \exp(-im\theta)$, and the non-adiabatic (kinetic) contribution δF_k is e.g. defined in Eqs. 4 and 5 of Ref. [3]. Here \mathcal{P}_ϕ is the toroidal canonical momentum which is conserved over the radial drift of a single particle. In the limit of zero radial drift excursion, or orbit width Δr , the adiabatic (or fluid) contribution is simply a result of convective ‘c’ motion perpendicular to the field line, $\delta F_c = -\underline{\xi}_\perp \cdot \underline{\nabla} F$. Meanwhile, δF_k is associated with the parallel dynamics, and is often referred to as the response due to kinetic-compressibility. In particular, replacing the drift kinetic treatment employed here with the ideal MHD model, one would substitute δF_k defined above with $\delta F_{knc} = -\gamma F \underline{\nabla} \cdot \underline{\xi}$, the non-convective ‘nc’ stabilising effect of compressibility. Assuming an isotropic equilibrium distribution function, taking a second velocity moment of $\delta F_c + \delta F_{knc}$ simply yields the MHD perturbed pressure $\delta P = -\underline{\xi}_\perp \cdot \underline{\nabla} P - \gamma P \underline{\nabla} \cdot \underline{\xi}$. The MHD model provides a very poor description of the parallel dynamics of energetic particles, and clearly cannot describe resonant wave-particle interaction. However, MHD is a good model of perpendicular dynamics. In particular, the perpendicular component of the MHD equation of motion, in which $\delta P_c = -\underline{\xi}_\perp \cdot \underline{\nabla} P$ (the second moment of δF_c) appears explicitly, describes the essential perpendicular dynamics of a hybrid kinetic-MHD treatment. Nevertheless, in addition to the well known non-convective effects associated with the kinetic response δF_k , finite orbit widths introduce additional relatively exotic effects in δF_f [4, 3]. As we will see, by expanding $\delta F_f = \delta F_{f0} + \delta F_{f1}$ with respect to orbit radial width Δr , we are able to identify the finite orbit correction associated with the adiabatic contribution [4, 3]:

$$\delta F_{f1} = -(Ze/m)(\underline{\xi} \cdot \underline{\nabla} \psi_p) \frac{\partial F_0 + F_1}{\partial \mathcal{P}_\phi} + \underline{\xi}_\perp \cdot \underline{\nabla} F_0. \quad (2)$$

where the equilibrium distribution $F = F_0 + F_1 + ..$ has also been expanded in Δr . It is in this correction that the effect of parallel velocity asymmetry on the internal kink mode arises, and,

we claim, the resulting observable affect on sawteeth.

In order to relate Eq. (2) to a potential energy δW , we recall that δW is defined in terms of the perturbed force $\underline{\delta \mathcal{F}}$ via $\delta W = -(1/2) \int d^3x \underline{\xi}_\perp^* \cdot \underline{\delta \mathcal{F}}$, where

$$\underline{\delta \mathcal{F}} = \underline{\delta j} \times \underline{B} + \underline{j} \times \underline{\delta B} - \nabla \cdot \underline{\delta P}.$$

Now, the fast ions primarily influence the linear perturbed force $\underline{\delta \mathcal{F}}$ through the perturbed pressure tensor $\underline{\delta P}$. The fast ion pressure tensor $\underline{\delta P}$ is of course obtained by evaluating the second velocity moments of δF , and results in,

$$\delta W = \frac{1}{2} m \int d^3x \int d^3v \underline{k} \cdot \underline{\xi}_\perp^* \left(v_\parallel^2 + \frac{v_\perp^2}{2} \right) \delta F_h. \quad (3)$$

To make progress we need to expand F in orders of the orbit width Δ_r , so that $F = F_0 + F_1 + \dots$. We note that another constant of motion, defined by \mathcal{P}_ϕ , is the temporal average of the particles' minor radius, \bar{r} , over a full toroidal transit, i.e. $\bar{r} = \tau_b^{-1} \int_0^{\tau_b} dt r(t)$, where τ_b is the bounce time, or transit time, for respectively trapped or passing particles. Writing $r(t) = \bar{r} + \Delta_r(t)$ we have,

$$F_0 = F(\mathcal{E}, \mu, \bar{r})|_{\bar{r} \rightarrow r} \quad \text{and} \quad F_1(\mathcal{E}, \mu, r) = -\Delta_r G_0(\mathcal{E}, \mu, r), \quad (4)$$

and

$$G_0(\mathcal{E}, \mu, r) = G(\mathcal{E}, \mu, \bar{r})|_{\bar{r} \rightarrow r} \quad \text{and} \quad G = \frac{\partial F}{\partial \bar{r}}, \quad (5)$$

with

$$\Delta_r = \frac{\sigma q}{r \Omega_c} (|v_\parallel| R - p R_0^2 q \omega_b), \quad (6)$$

where σ is the sign of v_\parallel , $p = 1$ for passing particles, $p = 0$ for trapped particles, $\omega_b = 2\pi/\tau_b$ and $\Omega_c = eZB_0/m$. Also, $\mathcal{E} = v^2/2$ is the kinetic energy, and $\mu = v_\perp^2/(2B)$. Defining $F^\pm = F(\sigma)$ and $G^\pm = G(\sigma)$ etc to separate the contributions of particles with respectively $v_\parallel > 0$ and $v_\parallel < 0$, one can now obtain various potential energy contributions (normalised as $\hat{\delta W} = \delta W / (2\pi^2 R_0 \xi^2 \varepsilon_1^2 B_0^2 / \mu_0)$) due to passing and trapped ions. Note that the the pitch angle $k^2 = (1 - \lambda B_0(1 - \varepsilon))/2\lambda B_0 \varepsilon$ is employed for trapped ions, and $y^2 = 1/k^2$ for passing ions, where $\lambda = \mu/\mathcal{E}$ and $\varepsilon = r/R_0$ the local inverse aspect ratio. We now go about solving for the adiabatic contribution, corresponding to Eq. (1). In order to separate zeroth order effects from finite orbit effects, we expand Eq. (1) about the flux label r . For this purpose we note that $\underline{\xi} \cdot \nabla \psi = r B_0 \xi_r / q(r)$ and $\partial/\partial \mathcal{P}_\phi = \Omega_c^{-1} (q(\bar{r})/\bar{r}) \partial/\partial \bar{r}$, $r/\bar{r} = 1 + (\Delta_r/r)$, $q(\bar{r})/q(r) = 1 - (\partial \Delta_r / \partial r)$, where $\partial \Delta_r / \partial r = \Delta_r s(r)/r$. This then yields

$$\delta F_f^\sigma = \delta F_{f0}^\sigma + \delta F_{f1}^\sigma \quad (7)$$

with the lowest order convective contribution:

$$\delta F_{f0}^\sigma = -\xi_r G_0^\sigma, \quad (8)$$

and the finite orbit correction:

$$\delta F_{f1}^\sigma = -\xi_r \frac{\Delta_r}{r} \left((2-s) G_0^\sigma - \frac{y^2}{2} (2-y^2) \frac{\partial G_0^\sigma}{\partial y^2} \Big|_r - \frac{\partial (r G_0^\sigma)}{\partial r} \Big|_{y^2} \right), \quad (9)$$

where it is important to highlight that $\partial G / \partial r|_\lambda = \partial G / \partial r|_{y^2} - (2-y^2)(y^2/2) \partial G / \partial y|_r$, must be taken into account when dealing with partial derivatives. We are reminded however, that G_0 ,

defined in Eq. (5), is the radial derivative of F , with λ kept constant, since $G = \partial F / \partial \bar{r} |_{\lambda}$. The last term in Eq. (9) is the only finite orbit term that contributes significantly to δW when the additional kinetic response δF_k is included [3]. By employing the leading order internal kink perturbation, assuming that the mode is close to marginal stability, such that $\xi_r = H[r_1 - r] \exp(-i\theta - i\phi - i\omega t)$ with H the Heaviside step function, we obtain [3]:

$$\delta \hat{W}_{r_1} = - \left(\frac{2}{\pi} \right)^{1/2} \frac{2}{\epsilon_1} \int_0^1 dy^2 \left(\frac{\epsilon_1 y^2}{2} - \frac{2G_1 + G_2}{K[y^2]} \right) \left(\frac{q}{\Omega_c} \right) \left(\frac{eT_{\perp}}{m} \right)^{1/2} \left(\frac{2\mu_0}{B_0^2} \right) (C^+ - C^-) \Big|_{r=r_1}, \quad (10)$$

where

$$C^{\sigma} = \left(\frac{eT_{\perp}}{m} \right)^{-1/2} \frac{(m/2)(\pi/2)^{3/2}}{[y^2 + \epsilon(2 - y^2)]^3} \int_0^{\infty} d\mathcal{E} (2\mathcal{E})^2 G_0^{\sigma},$$

is valid for an arbitrary distribution function. Here

$$G_1 = \frac{\epsilon}{2} \oint d\theta \cos \theta (1 - \epsilon \cos \theta) [1 - y^2 (\sin(\theta/2))^2]^{1/2} \quad \text{and} \quad G_2 = \frac{y^2}{4} \oint d\theta \frac{\cos \theta (1 - \epsilon \cos \theta)^2}{[1 - y^2 (\sin(\theta/2))^2]^{1/2}},$$

both of which can be written [3] in terms of complete elliptic integrals of the first kind $K[y^2]$ and second kind $E[y^2]$. Only particles with orbits that intersect r_1 contribute to $\delta \hat{W}_{r_1}$. Clearly the number of particles that do intersect increases with orbit width of a typical particle, and this in turn is determined by the particle energy. Consequently, δW_{r_1} is proportional to the characteristic orbit width (i.e. $T^{1/2}$) multiplied by the pressure gradient (essentially proportional to C^{σ}). Moreover, δW_{r_1} is zero for a symmetric distribution in v_{\parallel} at r_1 (for which $C^+ - C^- = 0$). We repeat that the parallel velocity asymmetry is introduced in the experiment via the deployment of toroidally propagating ICRF waves (+90 or -90 phasing using the JET antennas). Moreover, the gradient in the distribution function (G_0^{σ}) at r_1 can be varied extremely sensitively by moving the resonance position across r_1 . Experimentally this is achieved by slowly ramping the toroidal field, and proportionally, the plasma current. The final control parameter is the tail temperature, which determines the characteristic orbit width. This can be controlled experimentally by variation of the minority concentration while containing the fast ion pressure through keeping the RF power constant. It is pointed out here that the characteristics of δW_{r_1} have been compared [5] favourably with the results of the HAGIS code [12], and in particular, the contribution to δW due to finite orbit widths. This has been undertaken by simulations capable of isolating only the contribution to HAGIS of particles intersecting r_1 , and by variation of the radial gradient of the distribution and the direction and degree of asymmetry. In order to undertake accurate simulations without approximation of the SELFO [13] generated distribution function, we choose to model JET experiments using the HAGIS code, but we are confident in interpreting the results based on the physics indicated by Eq. (10) and the analysis that went into deriving it.

3. Simulations and Experimental Comparisons

We now address the experimental objective of generating negligible minority ion current in order to eliminate and avoid the traditional sawtooth control mechanism [7] involving the change the magnetic shear at $q = 1$. The asymmetry in toroidal wave number spectra, due to the antenna phasing, gives rise to Fisch currents [9] and currents due to preferential detrapping [10] of co and counter circulating ions. The SELFO code calculates these currents in addition to currents that are insensitive to antenna phasing which arise from the guiding centre drift orbits of predominantly trapped and barely passing ions. However, the plasma is dragged [9, 7] along with the fast ions, such that the total current is proportional to a drag coefficient j_d , giving $j_{tot} = j_h \times j_d$. The fast ion current is subject to momentum conservation, quasi-neutrality and the balance of collision rates of electrons on all ion species [9, 7], giving

$$j_d = 1 - \left[\frac{Z_h}{Z_{eff}} + \frac{m_h \sum_i Z_i n_i (1 - Z_i / Z_{eff})}{Z_h \sum_i n_i m_i} - G \left(\frac{Z_h}{Z_{eff}} - \frac{m_h \sum_i n_i Z_i^2}{Z_h Z_{eff} \sum_i n_i m_i} \right) \right], \quad (11)$$

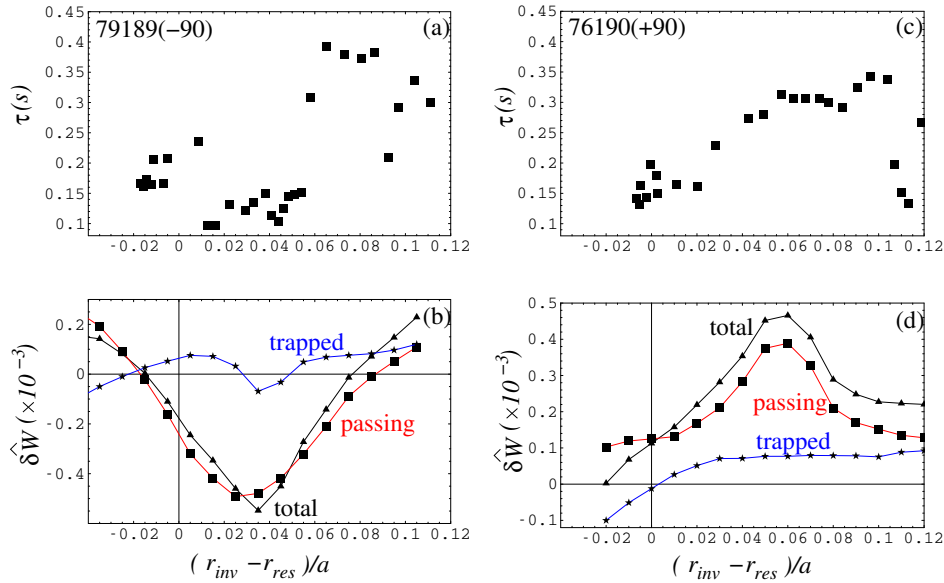


FIG. 3. Showing the comparison of internal kink stability modelling and RF sawtooth control experiments reported in Ref. [6]. (a) and (b) are the measured sawtooth period, and simulated δW contribution for 76189 (-90° phasing). (c) and (d) are the same but for 76190 ($+90^\circ$). Reproduced from Fig. 4 of Ref. [J. P. Graves, et al, Nucl. Fusion **50** 052002 (2010)]. Copyright rests with Euratom.

where $G = 1.46A(Z_{eff})\epsilon^{1/2}$, A is a weak function of Z_{eff} and i denotes ion species other than hot (h). In Ref. [6] it is shown that j_h has a dipole structure, with maximum current around 30 kA/m². Due to the minority ion mass number $m_h = 3$ and charge $Z_h = 2$, deuterium bulk ion population, carbon and beryllium impurities, and moderate $Z_{eff} \approx 1.8$, the effect of the plasma drag is to lower the net driven current density by at least 90% within the $q = 1$ surface, so that the change in the shear due to current drive is negligible. It is therefore concluded that the sawteeth were not controlled by the effect of ICRF current drive on s_1 . Moreover, that the trend in the sawteeth is opposite for $+90^\circ$ and -90° phasings rules out the possibility that the sawteeth were modified simply by the effect of localised electron heating.

It is now shown that sawteeth are modified by ICRH even for pulses with relatively low auxiliary power. Diagnostic neutral beams with a power of 1.4MW were used in pulses 76189, employing 3MW of ICRF with -90° phasing, and 76190, employing 2MW ICRF with $+90^\circ$ phasing, both with low concentration (up to 0.5%) minority ^3He . The toroidal magnetic field was ramped upwards from around 2.88T to 2.96T, and the plasma current was ramped proportionally. Figure 3 (a) and (b) plots the sawtooth period for 76189 and 76190 as a function of the ^3He resonance position relative to the measured inversion radius. It is seen that the sawtooth period is strongly modified as the resonance position is shifted relative to the sawtooth inversion radius. The pulse with -90° phasing exhibits a narrow window of sawtooth destabilisation, while the $+90^\circ$ phasing pulse exhibits the opposite. Employing the SELFO generated distribution function for pulses 76189 and 76190 in the drift kinetic code HAGIS [12], together with an MHD displacement supplied from linear ideal MHD numerical calculations, reveals the corresponding fast ion contribution to $\delta\hat{W}$ without recourse to approximation of wave and guiding centre interaction. Figure 3 (c) and (d) compares the observed signature of the sawtooth period with the fast ion potential energy when plotted with respect to the difference between the ^3He resonance position and the measured and the $q = 1$ radius. The narrow region over which the sawteeth are sensitive to the ICRF deposition, also visible in Fig. 3, is recovered by the simulations, which assume $r_1 = r_{inv}$. The sign of the RF ion $\delta\hat{W}$ contributions is consistent with the observed effect on the sawteeth, and the amplitude is larger than all other contributions

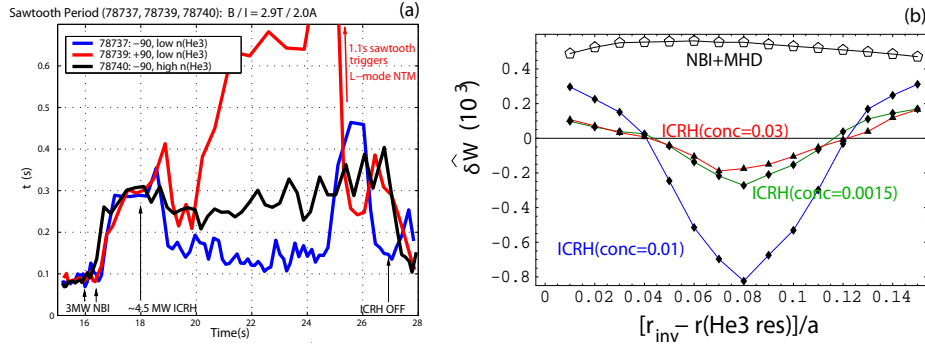


FIG. 4. In (a) the sawtooth period for 78737 (-90° phasing, low concentration ^3He), 78740 (-90° phasing, high concentration ^3He) and 78739 ($+90^\circ$ phasing, shown also in Fig. 1). In (b) stability ($\delta\hat{W}$) calculations, plotted with respect to $r_1 - r_{res}$. Curves with $n_h/n_e = 0.01$ and $n_h/n_e = 0.03$ correspond approximately to the conditions of 78737 and 78740 respectively. The NBI and MHD contributions are also shown. Reproduced from Figs. 5 and 6 of Ref. [J. P. Graves, et al, Nucl. Fusion **50** 052002 (2010)]. Copyright rests with Euratom.

to $\delta\hat{W}$ including the collisionless stabilisation from the NBI ions. We note from Fig. 3 that the response of the trapped ions is much less than the passing ion response, as expected from the mechanism of Eq. (10).

Furthermore, by exploiting the knowledge of the fast ion control mechanism derived in [3], it has been possible to reduce its effect, and the corresponding sawtooth control, thereby providing further experimental evidence in support of the theory. The aim is to reduce the finite orbit width of the fast ions, which scales with the hot ion temperature as $\Delta_r \propto T_h^{1/2}$. Referring e.g. to Stix [14], the hot ion temperature is proportional to the ICRH power, and inversely proportional to the minority ion concentration. Pulses with contrasting ^3He concentration exhibit the same signature with respect to the scan in resonance position, but the amplitude of the effect is reduced for increased concentration, as expected for the fast ion mechanism, and contrary to the current drive mechanism [7]. Pulse 78740 shown in Fig. 4 (a) employs approximately 4.5MW of -90° phasing ICRH with relatively high minority ^3He concentration (up to 3% of the electron density). This can be compared directly with the otherwise identical pulse 78737, detailed also in Fig. 2, employing -90° phasing with relatively low minority ^3He concentration (up to $n_h/n_e = 0.6\%$). The several-fold increase in ^3He concentration in 78740, relative to 78737, is consistent with the deliberate increased opening of the ^3He gas valve. The two pulses exhibit the same signature with respect to the scan in resonance position, but the amplitude of the effect is reduced for increased concentration, as expected for the fast ion mechanism, and contrary to the current drive mechanism [7] (currents remain negligible). Detailed verification [6] that the fast ion mechanism [3] is consistent with the experiments shown in Fig. 4 (b) is undertaken by SELFO/HAGIS simulations evaluating the stability of JET pulses 78737 and 78740. Figure 4 plots the ICRH ion contribution to $\delta\hat{W}$, upon variation of $r_1 - r_{res}$, for $n_h/n_e = 0.01$ and $n_h/n_e = 0.03$, relevant for 78737 and 78740 respectively. It is seen that the range in $r_1 - r_{res}$ over which ICRH has a destabilising effect is independent of concentration. Meanwhile, the strength of destabilisation of counter propagating ICRH waves on the internal kink mode is even more sensitive to concentration than would be expected from the simple relation $\Delta_r \propto (n_e/n_h)^{1/2}$. For $n_h/n_e = 0.01$ the effect of ICRH dominates stability, while for $n_h/n_e = 0.03$ the effect of ICRH is much smaller than the combined effect of NBI and MHD, as expected from experiments (Fig. 4 (a)). Finally, if the ^3He concentration is too low, minority power absorption is reduced, and enhanced minority ion energies lead to broader hot ion deposition, and losses, and a reduced impact on sawteeth, as indicated by the simulation in Fig. 4 (b) employing $n_h/n_e = 0.0015$.

4. Conclusions

This paper summarises a new mechanism [3] that has been proposed to explain the highly effective nature of sawtooth control using off-axis toroidally propagating ICRH. By developing an analytical treatment, it is shown that energetic passing ions influence the internal kink mode when the distribution of ions is asymmetric in v_{\parallel} . Such distributions are clearly a natural product of co or counter propagating ICRH waves. When a counter propagating wave is deposited sufficiently close to the $q = 1$ radius, r_1 , on the high field side, the fast ion effect is so strong that the internal kink mode is driven ideally unstable. Furthermore, it is shown that the response of the fast ions on the internal kink mode is very sensitive to the difference between the position of the RF resonance radius and r_1 . This is due to the fact that the only fast ions that contribute are those that intersect the $q = 1$ radius, and thus the mechanism is not diminished by integration over sharp features in the distributions' radial profile. Moreover, the mechanism can also explain sawtooth stabilisation with co-propagating waves on the high field side. With this theoretical model at hand, it was possible to design experiments [6] capable of testing the mechanism over various parameters, while eliminating other known control mechanisms. Choosing ^3He minority ensured that there would be minimal modification of the magnetic shear due to ICCD. Despite this, it was found that the sawtooth period was extremely sensitive to the RF resonance position relative to the $q = 1$ radius, as expected from the theory. Furthermore, more advanced experimental verification has been undertaken [6] by variation of the amplitude of the fast ion mechanism. In particular, by reducing the tail temperature, and therefore the orbit widths of the fast ions, via an increase in the ^3He concentration, it was verified that sawtooth control becomes less effective. In the present proceedings, these dedicated experiments are compared favourably with sophisticated modelling using the SELFO [13] code for the fast ion distribution function, and the HAGIS [12] code for the stability calculations. In these codes the physics of finite orbit widths are included in the calculations. Finally, that fast ions can so dramatically, and directly, affect sawteeth is encouraging for ^3He minority ICRH deployment in ITER, where control solely via the magnetic shear is expected to be more challenging [15].

Acknowledgements

This work, supported by the Swiss National Science Foundation, and by the EC under contract of Association between EURATOM and Confédération Suisse, was carried out within the framework of the European Fusion Development. The views and opinions expressed herein do not necessarily reflect those of the European Commission.

References

- [1] F. Porcelli, *et al* Plasma Phys. Control. Fusion **38** 2163 (1996)
- [2] I. T. Chapman, *et al*, Nucl. Fusion **50** 102001 (2010)
- [3] J. P. Graves, *et al*, Phys. Rev. Lett. **102**, 065005 (2009)
- [4] J. P. Graves, Phys. Rev. Lett. **92**, 185003 (2004)
- [5] I. T. Chapman, *et al*, Plasma Phys. Control. Fusion **50**, 045006 (2008)
- [6] J. P. Graves, *et al*, Nucl. Fusion **50** 052002 (2010)
- [7] V.P. Bhatnagar, *et al*, Nucl. Fusion **34**, 1579 (1994)
- [8] L.-G. Eriksson, *et al*, Phys. Rev. Lett. **92**, 235004 (2004)
- [9] N. J. Fisch, *et al*, Rev. Mod. Phys. **59**, 175 (1987)
- [10] T. Hellsten, J. Carlsson, L.-G. Eriksson, Phys. Rev. Lett. **74**, 3612 (1995)
- [11] P. Helander *et al*, Phys. Plasmas **4**, 2182 (1997)
- [12] S.D. Pinches, *et al*, Comp. Phys. Comm. **111**, 133 (1998)
- [13] J. Hedin, *et al*, Nucl. Fusion **42**, 527 (2002)
- [14] T. H. Stix, Nucl. Fusion **15**, 737 (1975)
- [15] M. Laxåback and T. Hellsten, Nucl. Fus. **45**, 1510 (2005)